Materials Chemistry and Physics 114 (2009) 595–598

Contents lists available at ScienceDirect

Materials Chemistry and Physics

journal homepage: www.elsevier.com/locate/matchemphys

Corrosion behaviors of austenitic Fe–30Mn–7Al–*x*Cr–1C alloys in 3.5% NaCl solution

Y.H. Tuan, C.S. Wang, C.Y. Tsai, C.G. Chao, T.F. Liu *

Department of Materials Science and Engineering, National Chiao Tung University, 1001 Ta Hsueh Road, Hsinchu 30049, Taiwan

ARTICLE INFO

Article history:
Received 28 May 2008
Received in revised form
18 September 2008
Accepted 2 October 2008

Keywords:
Alloy
Corrosion
Electrochemical techniques
Carbides

ABSTRACT

The corrosion behaviors of the as-quenched Fe–30 wt.%Mn–7 wt.%Al–*x* wt.%Cr–1 wt.%C alloys (*x* = 0, 3, 6 and 9) in 3.5% NaCl have been investigated. Passivation could be observed for all the alloys except for the alloy without Cr content. The corrosion potential (E_{corr}) and pitting potential (E_{pp}) increased pronouncedly with increasing Cr content up to 6 wt.%, and decreased as Cr content up to 9 wt.%. The decrease of E_{corr} and E_{pp} of the alloy containing 9 wt.% Cr was due to the formation of $(Fe,Mn,Cr)_7C_3$ carbides in the austenite matrix and on the grain boundaries. It is noted that the corrosion behaviors of the austenitic Fe–Mn–Al–Cr–C alloys with higher Cr (≥3 wt.%) content have never been reported in previous literatures.
© 2008 Elsevier B.V. All rights reserved.

1. Introduction

The austenitic Fe–Mn–Al–C quaternary alloys have many advantages, such as low cost, low density, high strength, high toughness, and good oxidation resistance [1–6]. However, the corrosion resistance of the austenitic Fe–Mn–Al–C alloys in aqueous environments was not adequate for applications in industry [5–13]. Therefore, many researchers tried to improve the corrosion resistance of the austenitic Fe–Mn–Al–C alloys by adding chromium and decreasing carbon content [6,9,14–17]. Since Cr and C are ferrite and austenite formers in ferrous alloys, respectively, the Fe–Mn–Al–Cr–C alloys with higher Cr and lower C contents consist of (austenite + ferrite) dual-phases. Some literatures showed that Fe–(21.5–27.7) wt.%Mn–(8.9–9.9) wt.%Al–(3.1–6.2) wt.%Cr–(0.33–0.42) wt.%C alloys exhibited austenite and ferrite dual-phases, and the mechanical properties of the dual-phase Fe–Mn–Al–Cr–C alloys were far inferior to those of austenitic ones. In order to obtain full austenitic structure, a proper combination of chromium and carbon contents was treated. In the previous studies [5,6], it was reported that the Fe–(29.5–31.3) wt.%Mn–(8.4–8.9) wt.%Al–(2.6–2.8) wt.%Cr–(0.98–1.06) wt.%C alloys had a single-phase austenite, and the corrosion resistance of the austenitic Fe–Mn–Al–Cr–C alloys was indeed superior to that of the austenitic Fe–Mn–Al–C or dual-phase Fe–Mn–Al–Cr–C alloys. However, to date, information concerning the corrosion behaviors of the austenitic Fe–Mn–Al–Cr–C alloys with higher Cr (≥3 wt.%) content is very deficient. In this study, the electrochemical corrosion properties of four austenitic Fe–30 wt.%Mn–7 wt.%Al–1 wt.%C alloys with 0, 3, 6 and 9 wt.% Cr contents in 3.5% NaCl solution were investigated to evaluate the effects of Cr content on the corrosion resistance.

2. Experimental procedure

The chemical compositions of the alloys are shown in Table 1. The alloys were prepared by melting commercial pure Fe, Mn, Al, Cr and carbon powder in an induction furnace under a controlled protective argon atmosphere. The melt was cast into 30 mm × 50 mm × 200 mm ceramic shell mold. After being homogenized at 1473 K for 24 h, the ingots were sectioned into 12 mm × 12 mm × 5 mm slices. These slices were subsequently solution heat-treated in vacuum furnace at 1373 K for 2 h and then rapidly quenched into room-temperature water. Potentiodynamic polarization curves were measured in 3.5% NaCl solution at 298 K. Electrochemical polarization curves were obtained by using an EG&G Princeton Applied Research Model 273 galvanostat/potentiostat. Specimens with an exposed surface area of ~1 cm^2 were ground with 2000-grit SiC paper and then with 1.5 μm Al_2O_3 powder, washed in distilled water and rinsed in acetone prior to passivation. Potentiodynamic polarization curves were obtained at a potential scan rate of 5 mV s^{-1} from −1 to 0.5 V. The concentration of elements in the passive film was examined by Auger electron spectroscopy (AES) and X-ray photoelectron spectroscopy (XPS). As well known, the composition quantification of AES is very poor due to matrix effect, peaks overlapping and surface roughness, etc. However, the depth profiling is one of the most important and convenient application of AES for analyzing the composition of thin surface layer. Therefore, the depth profiling of AES is an appropriate and effective method for analyzing the composition distributions of the passive film in this experiment [18,19]. Microstructures were examined by using optical microscopy and transmission electron microscopy (TEM). TEM specimens were prepared by means of a double-jet electropolisher with an electrolyte of 15% perchloric acid, 25% acetic

* Corresponding author. Tel.: +886 3 5131288; fax: +886 3 5713987.
E-mail addresses: tfliu@cc.nctu.edu.tw, yixduan@gmail.com, phyxsiusmilo@gmail.com (T.F. Liu).

0254-0584/$ – see front matter © 2008 Elsevier B.V. All rights reserved.
doi:10.1016/j.matchemphys.2008.10.009

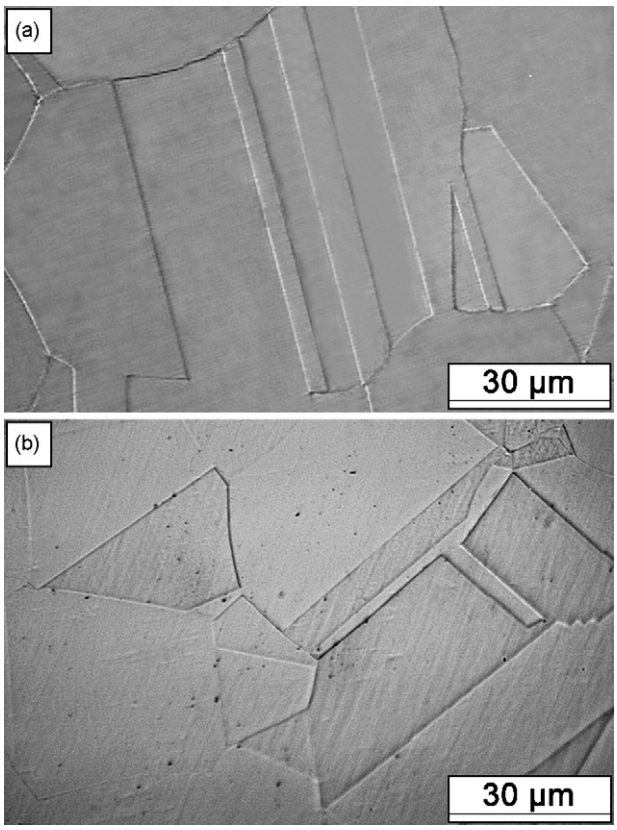

Fig. 1. Optical micrographs of the Fe–30 wt.%Mn–7 wt.%Al–(6, 9) wt.%Cr–1 wt.%C alloys. (a) 6 wt.%Cr, and (b) 9 wt.%Cr.

Table 1
Chemical compositions of the present alloys (wt.%).

Alloy	Mn	Al	Cr	C	Fe
A(0Cr)	29.18	7.05	0	0.96	Bal.
B(3Cr)	29.92	7.12	3.01	1.04	Bal.
C(6Cr)	30.12	7.06	5.96	1.01	Bal.
D(9Cr)	30.02	7.08	9.05	0.98	Bal.

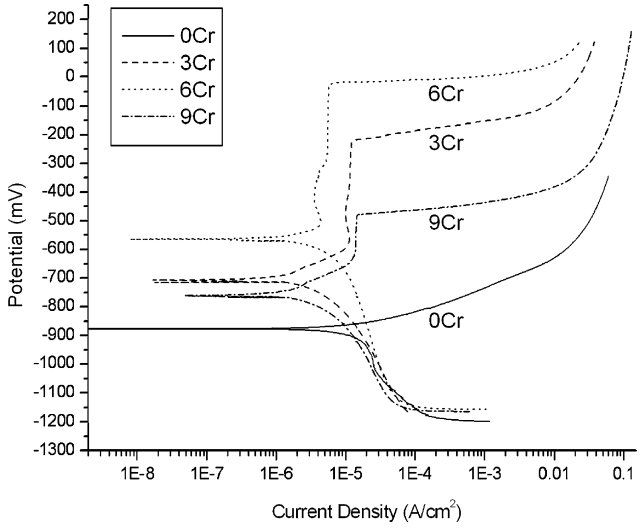

Fig. 2. Potentiodynamic polarization curves for the five Fe–30 wt.%Mn–7 wt.%Al–(0, 3, 6, and 9) wt.%Cr–1 wt.%C alloys in 3.5% NaCl solution.

Table 2
The electrochemical parameters from potentiodynamic polarization curves for the Fe–30 wt.%Mn–7 wt.%Al–(0, 3, 6 and 9) wt.%Cr–1 wt.%C alloys in 3.5% NaCl solution.

Alloy	Electrochemical parameters from polarization curves			
	E_{corr} (mV)	E_{cr} (mV)	E_{pp} (mV)	Ip (A cm^{-2})
A(0Cr)	−877	–	–	–
B(3Cr)	−712	−588	−224	4.1E−05
C(6Cr)	−556	−518	−27	5.75E−06
D(9Cr)	−754	−599	−472	1.78E−05

E_{corr}, corrosion potential; E_{cr}, critical potential for active–passive transition; E_{pp}, pitting potential; Ip, passive current density, minimum value.

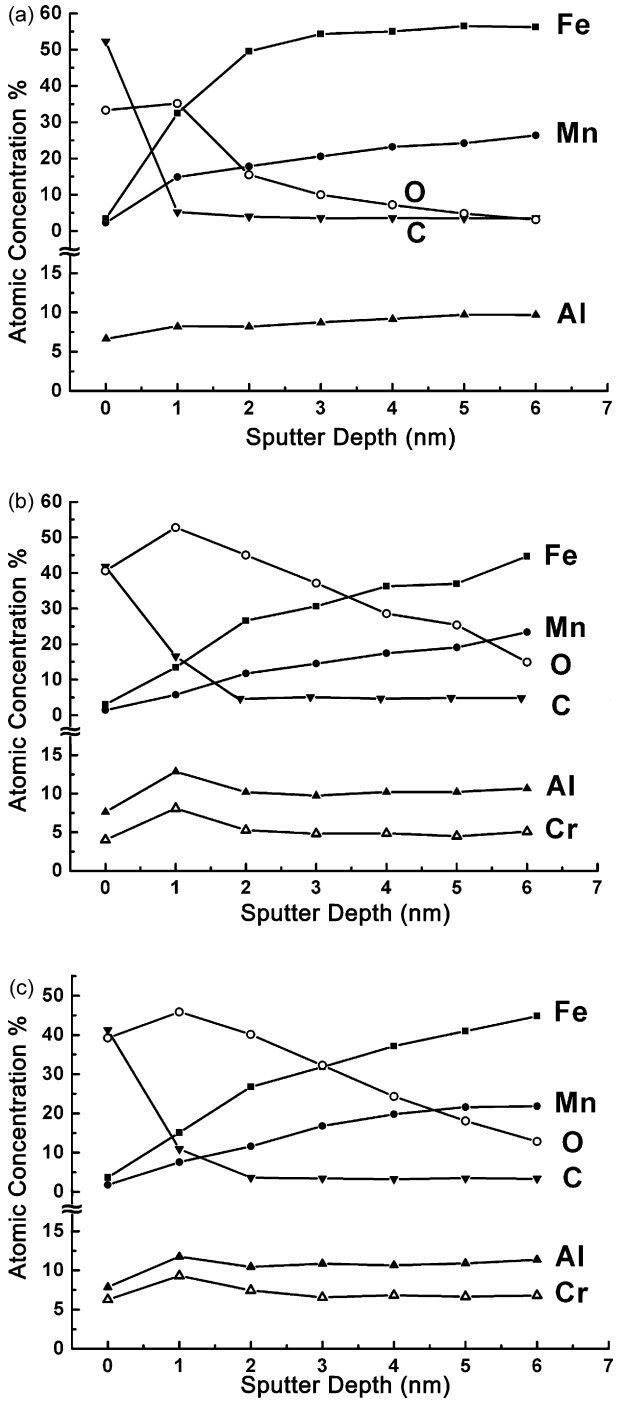

Fig. 3. AES depth profiles for the passive film of the Fe–30 wt.%Mn–7 wt.%Al–(0, 6, and 9) wt.%Cr–1 wt.%C alloys. (a) 0 wt.%Cr, (b) 6 wt.%Cr, and (c) 9 wt.%Cr.

Download English Version:

https://daneshyari.com/en/article/1525819

Download Persian Version:

https://daneshyari.com/article/1525819

Daneshyari.com